REPORT NO.
UCB/SEMM-97/09

STRUCTURAL ENGINEERING
MECHANICS AND MATERIALS

A MIXED-ENHANCED STRAIN METHOD: FINITE DEFORMATION PROBLEMS

BY

ERIC P. KASPER

AND

ROBERT L. TAYLOR

AUGUST 1997

DEPARTMENT OF CIVIL AND ENVIRONMENTAL ENGINEERING
UNIVERSITY OF CALIFORNIA, BERKELEY

A Mixed-Enhanced Strain Method: Finite Deformation Problems

Eric P. Kasper and Robert L. Taylor

Department of Civil and Environmental Engineering
University of California at Berkeley, Berkeley, CA 94720-1710
Report No.: UCB/SEMM-97/09

Abstract

A general formulation of an assumed strain method in the context of mixed finite elements is presented. A mixed strain field, to which an enhancement is added, results in a formulation which produces coarse mesh accuracy in bending dominated problems and locking-free response in the near incompressible limit. Due to the mixed fields present, variational stress recovery is also available. Also, the construction of the formulation is such that the mixed parameters may be obtained explicity and the resulting finite element arrays obtain full rank using standard order quadrature. In this paper our attention is focused on finite deformation problems in solid mechanics. Specifically, we investigate the proposed formulation in the setting of incompressible hyperelasticity . Representative simulations illustrate the performance of the formulation.

1. Introduction

The key idea of the present work is the parametrization of the deformation gradient in terms of a mixed and an enhanced deformation gradient from which a consistent formulation is derived using standard mixed method techniques. This methodology allows for a formulation which has standard order quadrature and variationally recoverable stresses, hence circumventing difficulties which arise in other *assumed strain* methods. To the authors' knowledge, the formulation presented herein has not been currently explored. Developments of the formulation are cast within the area of non-linear elasticity.

It is well known that finite elements based upon low order isoparametric displacement formulations exhibit poor performance in bending and locking in the nearly incompressible limit. Recent formulations which exhibit improved coarse mesh accuracy fall into two categories namely *assumed stress* and *assumed strain* methods. Our formulation is addressed in the context of *assumed strain* methods which are preferred to their *assumed stress* counterparts, due to their natural compatibility with the strain drive format.

One of the first developments in the linear regime was by WILSON ET. AL. [1973] who proposed the addition of internal incompatible displacement modes of quadratic distribution to enhance bending performance of quadrilateral elements. Subsequently, it was discovered that the element failed the patch test for an arbitrary quadrilateral. TAYLOR ET. AL. [1976] proposed modifications to Wilson's original formulation which allowed for satisfaction of the patch test for arbitrary configurations. In later developments SIMO & RIFAI [1990] present a systematic development of a class of *assumed strain* methods. They provide the framework for the development of low order elements possessing improved performance in bending dominated problems in the context of small strains. Issues related to convergence and stability are also presented. Extensions were made by SIMO &

ARMERO [1992] to the enhanced strain formulation to incorporate geometrical nonlinearities. They discussed the appearance of hourglass modes for highly strain regimes. The appearance of the modes was analyzed by WRIGGERS & REESE [1996]. REESE & WRIGGERS [1995] further discuss these spurious modes and proposed a stabilization technique, but unfortunately a general solution remains unknown. Improvements were made for the three dimensional formulation of SIMO & ARMERO [1992] by SIMO ET. AL. [1993] which incorporated modifications to the tri-linear shape functions, additional enhanced modes and an increased quadrature rule. The resulting element yielded a locking-free response in the incompressible limit and improved bending characteristics for both geometrically linear and nonlinear problems. Other approaches incorporating the effect of geometric nonlinearities include a co-rotational approach by CRISFIELD ET. AL. [1995], the work of KORELC & WRIGGERS [1996] which introduce additional orthogonality conditions which, if fulfilled, yield a stable enhanced element and the recent developments of GLASER & ARMERO [1996] which make two different extensions to the work of SIMO ET. AL. [1993]. In the first formulation they symmetrized the original enhanced interpolation of SIMO ET. AL. [1993] while the second formulation makes use of the transpose of the enhanced interpolation fields. These attempts resulted in elements which overcame deficiencies in highly strained compressive regimes. The present formulation also overcomes these deficiencies without the need for additional enhanced modes and uses standard order quadrature.

The paper is outlined as follows. In §2, basic notation is presented and a general formulation of a three field functional is given along with the strong form of the problem. The notion of the mixed-enhanced displacement gradient is introduced in §3 along with finite element approximations and interpolants for the mixed independent fields. Residual equations are then obtained, from which a numerical formulation is presented in the context of a Newton method. Representative numerical simulations are presented in §4 for the case of plane strain and three dimensional hyperelasticity. Finally, in §5 conclusions are drawn.

2. General Formulation

This section examines the proposed formulation in the setting of finite elasticity. We begin by an introduction to the basic notation and then summarize a three-field Hu-Washizu functional, WASHIZU [1982]. Finally, we present the resulting field equations, to be used subsequently for the finite element formulation.

2.1. Notation

The open set $\Omega \subset \mathbb{R}^n (n = 1, 2 \text{ or } 3)$ with smooth boundary $\partial\Omega$ represents a bounded reference configuration $\mathcal{B}$ for the continuum body. Identify a material point $X \in \bar{\Omega}$ with its position vector $\boldsymbol{X}$ relative to the standard basis in $\mathbb{R}^n$. We admit the decomposition of the boundary into two parts: $\Gamma_\varphi \subset \partial\Omega$ where the motion is prescribed as $\varphi = \bar{\varphi}$ and $\Gamma_t \subset \partial\Omega$ where the traction vector is prescribed as $\boldsymbol{P}\boldsymbol{N} = \bar{\boldsymbol{t}}$ subject to

$$\partial\Omega = \overline{\Gamma_\varphi \cup \Gamma_t} \quad \text{and} \quad \Gamma_\varphi \cap \Gamma_t = \emptyset \,. \tag{2.1}$$

In the above $\boldsymbol{P}$ is the 1st Piola-Kirchhoff stress tensor and $\boldsymbol{N}$ is the outward normal field to the boundary of the reference configuration. Upon deformation the material point X is mapped into a spatial position $\boldsymbol{x}$ by means of a single-valued continuously differentiable mapping function $\boldsymbol{\varphi} : \Omega \to \mathbb{R}^n$ defined as[1]

$$\boldsymbol{x} = \boldsymbol{\varphi}(\boldsymbol{X}) = \boldsymbol{X} + \boldsymbol{u}(\boldsymbol{X}) \ , \tag{2.2}$$

where $\boldsymbol{u}$ is the displacement field and $\boldsymbol{\varphi} \in \mathcal{U}$, $\mathcal{U}$ being the space of admissible motions written as

$$\mathcal{U} = \left\{ \boldsymbol{\varphi} : \Omega \to \mathbb{R}^n \mid \boldsymbol{\varphi} \in W^{1,p}(\Omega) \text{ and } \boldsymbol{\varphi} = \bar{\boldsymbol{\varphi}} \text{ on } \Gamma_{\varphi} \right\} \tag{2.3}$$

where $p \geq 2$ is dependent on the growth conditions of the stored energy function, see CIARLET [1988] for further details. we denote the deformation gradient and jacobean of the motion as

$$\boldsymbol{F} = \text{Grad}\,[\boldsymbol{\varphi}] = \frac{\partial \boldsymbol{\varphi}}{\partial \boldsymbol{X}} \quad \text{with} \quad J = \det \boldsymbol{F} > 0 \tag{2.4}$$

where $\boldsymbol{F} \in \mathcal{M}$ and $\mathcal{M}$ is defined as

$$\mathcal{M} = \left\{ \mathbf{F} : \Omega \to \mathbb{R}^{n \times n} \mid F_{iI} \in L^2(\Omega) \right\} \ . \tag{2.5}$$

2.2. Three-Field Variational Formulation

For the proposed formulation we use a Hu-Washizu type variational principle in which the motion $\boldsymbol{\varphi} \in \mathcal{U}$, the deformation gradient $\widetilde{\boldsymbol{F}} \in \mathcal{M}$ and the first Piola-Kirchhoff stress tensor $\widetilde{\boldsymbol{P}} \in \mathcal{M}$ are regarded as the independent variables. The proposed three-field functional $\Pi : \mathcal{U} \times \mathcal{M} \times \mathcal{M} \to \mathbb{R}$ may be expressed as

$$\Pi(\boldsymbol{\varphi}, \widetilde{\boldsymbol{F}}, \widetilde{\boldsymbol{P}}) = \int_{\Omega} \left[W(\boldsymbol{X}, \widetilde{\boldsymbol{F}}) + \widetilde{\boldsymbol{P}} \cdot (\text{Grad}\,[\boldsymbol{\varphi}] - \widetilde{\boldsymbol{F}}) \right] dV \ + \ \Pi_{ext} \tag{2.6}$$

where $W(\boldsymbol{X}, \widetilde{\boldsymbol{F}})$ is an objective stored energy function and for conservative external loading

$$\Pi_{ext}(\boldsymbol{\varphi}) = - \int_{\Omega} \boldsymbol{b} \cdot \boldsymbol{\varphi} \ dV - \int_{\Gamma_t} \bar{\boldsymbol{t}} \cdot \boldsymbol{\varphi} \ dS \tag{2.7}$$

in which $\boldsymbol{b} : \Omega \to \mathbb{R}^n$ is the reference body force per unit volume.

We may state the solution of (2.6) as: Find $\boldsymbol{\varphi}$, $\widetilde{\boldsymbol{F}}$ and $\widetilde{\boldsymbol{P}}$, with $\boldsymbol{\varphi}$ satisfiying the Dirichlet boundary condition $\boldsymbol{\varphi} = \bar{\boldsymbol{\varphi}}$ on Γ_{φ}, which make the Hu-Washizu functional $\Pi(\boldsymbol{\varphi}, \widetilde{\boldsymbol{F}}, \widetilde{\boldsymbol{P}})$ stationary for all admissible variations $\delta\boldsymbol{\varphi} \in \mathcal{V}$, $\delta\widetilde{\boldsymbol{F}} \in \mathcal{M}$ and $\delta\widetilde{\boldsymbol{P}} \in \mathcal{M}$. Where $\mathcal{V}$ is the space of admissible variations of the motion written as

$$\mathcal{V} = \left\{ \delta\boldsymbol{\varphi} : \Omega \to \mathbb{R}^n \mid \delta\boldsymbol{\varphi} \in W^{1,p}(\Omega) \text{ and } \delta\boldsymbol{\varphi} = \mathbf{0} \text{ on } \Gamma_{\varphi} \right\} \ . \tag{2.8}$$

[1] Note the reference and spatial coordinate frames are chosen to coincide and share a common basis.

Since there are no explicit constraints on $\widetilde{\boldsymbol{F}}$ and $\widetilde{\boldsymbol{P}}$ we may take the variations $\delta\widetilde{\boldsymbol{F}}$ and $\delta\widetilde{\boldsymbol{P}}$ to be contained within $\mathcal{M}$ as defined in (2.5).

The stationary point of Π is obtained by setting to zero the first variation of (2.6) with respect to the three independent fields. Accordingly

$$\begin{aligned}
&\int_\Omega \operatorname{Grad}[\delta\boldsymbol{\varphi}] \cdot \widetilde{\boldsymbol{P}}\, dV + \delta\Pi_{ext} = 0 \\
&\int_\Omega \delta\widetilde{\boldsymbol{F}} \cdot \left(\frac{\partial W}{\partial \widetilde{\boldsymbol{F}}} - \widetilde{\boldsymbol{P}}\right)\, dV = 0 \\
&\int_\Omega \delta\widetilde{\boldsymbol{P}} \cdot \left(\operatorname{Grad}[\boldsymbol{\varphi}] - \widetilde{\boldsymbol{F}}\right)\, dV = 0\ .
\end{aligned} \tag{2.9}$$

for all admissible variations $\delta\boldsymbol{\varphi} \in \mathcal{V}$, $\delta\widetilde{\boldsymbol{F}} \in \mathcal{M}$ and $\delta\widetilde{\boldsymbol{P}} \in \mathcal{M}$.

Assuming regularity of the solution, using the divergence theorem along with standard arguments of the calculus of variations and assuming the integrand is well behaved yield the following Euler-Lagrange equations

$$\left.\begin{aligned}
\operatorname{Div}\widetilde{\boldsymbol{P}} + \boldsymbol{b} &= \boldsymbol{0} \\
\frac{\partial W}{\partial \widetilde{\boldsymbol{F}}} - \widetilde{\boldsymbol{P}} &= \boldsymbol{0} \\
\operatorname{Grad}[\boldsymbol{\varphi}] - \widetilde{\boldsymbol{F}} &= \boldsymbol{0}
\end{aligned}\right\} \qquad \text{in } \Omega \tag{2.10}$$

and the traction boundary condition

$$\widetilde{\boldsymbol{P}}\boldsymbol{N} = \bar{\mathbf{t}} \quad \text{on } \Gamma_t\ . \tag{2.11}$$

Equations (2.10) and (2.11) together with the requirement $\boldsymbol{\varphi} = \bar{\boldsymbol{\varphi}}$ on Γ_φ constitute the strong form of the local boundary value problem in the setting of finite elastostatics.

3. Finite Element Approximations

In this section we outline the interpolates used for the field variables, from which the mixed strain and stress fields are constructed in terms of nodal parameters as well as internal element parameters. Using the mixed strain field we construct an approximation to the three-field variational formulation. We then use the stationary condition to yield a reduced set of nonlinear equations, which are then linearized. From these equations finite element arrays are formulated. Finally, we outline a procedure for implementation of the formulation.

3.1. Finite Element Interpolations for the Field Variables

We begin by a discretization of the given reference domain Ω into a collection of polygonal shaped subdomains, $\bar{\Omega}_e$ such that $\Omega \approx \Omega^h = \bigcup_e \bar{\Omega}_e$ where $\bar{\Omega}_e$ is the closure of an individual element. Note that the collection is an approximation of the actual domain Ω. We admit the decomposition of the approximation to the boundary as $\partial\Omega \approx \partial\Omega^h = \overline{\Gamma^h_{\boldsymbol{\varphi}} \cap \Gamma^h_t}$ and $\Gamma^h_{\boldsymbol{\varphi}} \cup \Gamma^h_t = \emptyset$.

For isoparametric finite elements we define the reference geometry $\mathbf{X}^h \in \mathbb{R}^n$ and displacement field $\mathbf{u}^h \in \mathcal{U}^h$ over a typical element $\bar{\Omega}_e$ in the form

$$\mathbf{X}^h = \sum_{I=1}^{nen} N_I(\boldsymbol{\xi})\, \widehat{\mathbf{X}}^I \quad \text{and} \quad \mathbf{u}^h = \sum_{I=1}^{nen} N_I(\boldsymbol{\xi})\, \widehat{\mathbf{u}}^I \ , \tag{3.1}$$

where $N_I(\boldsymbol{\xi})$ are the standard isoparametric shape functions associated with node I, nen is the number of nodes on element $\bar{\Omega}_e$, h is a characteristic length of element $\bar{\Omega}_e$ and $\widehat{\mathbf{u}}^h, \widehat{\mathbf{X}}^h \in \mathbb{R}^n$, see ZIENKIEWICZ & TAYLOR, [1989] or HUGHES, [1987] for further details. The deformation gradient is then expressed by the standard relation

$$\boldsymbol{F} = \mathrm{Grad}\,[\boldsymbol{\varphi}] = \boldsymbol{I} + \mathrm{Grad}\,[\boldsymbol{u}] = \boldsymbol{I} + \sum_{I=1}^{nen} \mathrm{Grad}\, N_I \widehat{\boldsymbol{u}}^I \tag{3.2}$$

For the approximate problem we introduce the space $\mathcal{U}^h$ as a finite-dimensional approximation of $\mathcal{U}$, accordingly the space of admissible motions maybe written as

$$\mathcal{U}^h = \left\{ \boldsymbol{\varphi}^h : \Omega \to \mathbb{R}^n \mid \boldsymbol{\varphi}^h \in W^{1,p}(\Omega) \text{ and } \boldsymbol{\varphi}^h = \bar{\boldsymbol{\varphi}}^h \text{ on } \Gamma_\varphi \right\} \tag{3.3}$$

Lastly, the space $\mathcal{M}^h$, which contains the approximations to the stress and deformation gradient, is a finite-dimensional approximation of $\mathcal{M}$ given by

$$\mathcal{M}^h = \left\{ \boldsymbol{H}^h \mid H^h_{ij} \in L^2(\Omega^h) \right\} \ . \tag{3.4}$$

3.1.1. Mixed Approximations. The key idea for the mixed stress and deformation fields is to develop interpolates in the natural or isoparametric space and transform the results to the physical space. Based on requirements of tensor calculus, SOKOLNIKOFF, [1964], we use the following transformation relations for the stress tensor and deformation gradient

$$\mathcal{P}_{\alpha\beta}(\boldsymbol{\xi}, \boldsymbol{\beta}) = \tilde{\boldsymbol{P}}_{iI} \boldsymbol{F}_{iA} \boldsymbol{T}_{A\alpha} \boldsymbol{T}_{I\beta} \tag{3.5}$$

and

$$\mathcal{F}_{\alpha\beta}(\boldsymbol{\xi}, \boldsymbol{\beta}) = \tilde{\boldsymbol{F}}_{iI} (\boldsymbol{F}_{iA})^{-1} (\boldsymbol{T}_{A\alpha})^{-1} (\boldsymbol{T}_{I\beta})^{-1} \tag{3.6}$$

where $\mathcal{P}$ and $\mathcal{F}$ are the stress and deformation gradient in the isoparametric space, respectively. The above are defined so that $\mathcal{P} : \mathcal{F} = \tilde{\boldsymbol{P}} : \tilde{\boldsymbol{F}}$.

Let $\square$ denote the parent domain in the isoparametric space $\boldsymbol{\xi}$. Utilizing the mapping $\boldsymbol{X} : \square \rightarrow \Omega_e$ the Jacobian and the Jacobian determinant are expressed as

$$J_{I\alpha}(\boldsymbol{\xi}) = \frac{\partial X^I}{\partial \xi^\alpha} \quad \text{and} \quad j = \det J_{I\alpha} \ . \tag{3.7}$$

For the present formulation $\boldsymbol{T}$ and $\boldsymbol{F}$ used in (3.5) and (3.6) are averaged over the element Ω_e. This will permit direct inclusion of constant states, minimize the order of quadrature needed to evaluate the residual and tangent arrays and also reduce problems associated with initially distorted elements. The average quantities are denoted as

$$\boldsymbol{T} = \frac{1}{\Omega_e} \int_{\Omega_e} \boldsymbol{J}(\boldsymbol{\xi}) \, dV \quad \text{and} \quad \boldsymbol{F}_0 = \frac{1}{\Omega_e} \int_{\Omega_e} \boldsymbol{F} \, dV \ . \tag{3.8}$$

Substituting (3.8) into (3.5) and (3.6) yields the transformation of the fields $(\mathcal{P}, \mathcal{F})$ in the isoparametric space to the fields $(\tilde{\boldsymbol{P}}, \tilde{\boldsymbol{F}})$ in the physical space

$$\mathcal{P}(\boldsymbol{\xi}, \boldsymbol{\gamma}) = \boldsymbol{T}^T \boldsymbol{F}_0^T \tilde{\boldsymbol{P}} \boldsymbol{T} \quad \text{and} \quad \mathcal{F}(\boldsymbol{\xi}, \boldsymbol{\beta}) = \boldsymbol{T}^{-1} \boldsymbol{F}_0^{-1} \tilde{\boldsymbol{F}} \boldsymbol{T}^{-T} \ . \tag{3.9}$$

Remark 3.1.

1. The need for the deformation gradient in (3.5) and (3.6) which automatically comes from the tensor transformation, will ensure that the resulting stress and deformation gradient are objective when subjected to a superposed rigid body motion.
2. Alternatively, the Jacobian can be evaluated at the centroid, as originally suggested by PIAN & SUMIHARA, [1985] and TAYLOR *et al.*, [1976]. Note for two dimensions the average and centroidal Jacobians are identical.
3. Since the above transformation relations for the stress and strain are typically a measure of the isoparametric and physical space alternative transformations are admissible. Numerical observation by GLASER & ARMERO, [1996] and WRIGGERS & REESE, [1996] and confirmed during the developments of the present work show that replacing $\boldsymbol{J}$ by $\boldsymbol{J}^{-T}$ in $(3.8)_1$ results in transformation relations which are superior for the class of problems examined.

We next assume there exist linear maps $\mathcal{E}_1(\boldsymbol{\xi}, \cdot)$ and $\mathcal{E}_2(\boldsymbol{\xi}, \cdot)$ for which the fields $(\mathcal{P}, \mathcal{F})$ in the isoparametric space may be expressed as:

$$\begin{aligned} \mathcal{P}(\boldsymbol{\xi}, \boldsymbol{\beta}) &= \widehat{\boldsymbol{\beta}}_0 + \mathcal{E}_1(\boldsymbol{\xi}, \boldsymbol{\beta}) \\ \mathcal{F}(\boldsymbol{\xi}, \boldsymbol{\gamma}) &= \widehat{\gamma}_0 + \frac{1}{j} \left[\mathcal{E}_1(\boldsymbol{\xi}, \boldsymbol{\gamma}) + \mathcal{E}_2(\boldsymbol{\xi}, \boldsymbol{\alpha}) \right] \end{aligned} \tag{3.10}$$

where $\widehat{\boldsymbol{\beta}}_0$, $\boldsymbol{\beta}$, $\widehat{\gamma}_0$ and $\boldsymbol{\gamma}$ are parameters and $\mathcal{E}_1(\boldsymbol{\xi}, \boldsymbol{\gamma})$ and $\mathcal{E}_2(\boldsymbol{\xi}, \boldsymbol{\alpha})$ denote linear forms

$$\mathcal{E}_1(\boldsymbol{\xi}, \boldsymbol{\gamma}) = \sum_{k=1}^{n} \mathcal{E}_{k1}(\boldsymbol{\xi}) \gamma_k \quad \text{and} \quad \mathcal{E}_2(\boldsymbol{\xi}, \boldsymbol{\alpha}) = \sum_{k=1}^{m} \mathcal{E}_{k2}(\boldsymbol{\xi}) \alpha_k$$

where n and m are the number of parameters for the mixed and enhanced fields, respectively.

We construct the approximations $\mathcal{E}_1$ and $\mathcal{E}_2$ such that

$$\int_{\square} \mathcal{E}_1(\cdot)\, d\square = 0\ , \qquad \int_{\square} \mathcal{E}_2(\cdot)\, d\square = 0 \quad \text{and} \quad \int_{\square} \mathcal{E}_1(\cdot)\mathcal{E}_2(\cdot)\, d\square = 0\ . \tag{3.11}$$

The relations in (3.11) are used subsequently to decouple and solve for the element parameters of the mixed stress and strain.

Remark 3.2.

1. The mapping $\mathcal{E}_2(\boldsymbol{\xi}, \boldsymbol{\alpha})$ with its associated element parameters, $\boldsymbol{\alpha}$ were added to $(3.10)_2$ for two reasons: a) to improve performance in nearly incompressible regions, b) and to improve coarse mesh accuracy in bending dominated regimes.
2. Note the strain field in (3.10) has more parameters than the stress, hence we adopt the phrase *mixed-enhanced strain* as an extension of the terminology introduced by Simo & Rifai, [1990].

For two and three dimensional problems employing 4-node quadrilateral and 8-node hexahedral elements the maps $\mathcal{E}_1(\boldsymbol{\xi}, \cdot)$ and $\mathcal{E}_2(\boldsymbol{\xi}, \cdot)$ are given in Tables 3.1 and 3.2 below, respectively. The independent components are ordered in standard Voigt notation as:

Table 3.1 Two Dimensional Interpolations

i	j	$[\mathcal{E}_1(\boldsymbol{\xi}, \boldsymbol{\gamma})]_{ij}$	$[\mathcal{E}_2(\boldsymbol{\xi}, \boldsymbol{\alpha})]_{ij}$
1	1	$\xi_2\gamma_1$	$\xi_1\alpha_1$
2	2	$\xi_1\gamma_2$	$\xi_2\alpha_2$
1	2	0	0
2	1	0	0

Table 3.2 Three Dimensional Interpolations

i	j	$[\mathcal{E}_1(\boldsymbol{\xi}, \boldsymbol{\gamma})]_{ij}$	$[\mathcal{E}_2(\boldsymbol{\xi}, \boldsymbol{\alpha})]_{ij}$
1	1	$\xi_2\gamma_1 + \xi_3\gamma_2 + \xi_2\xi_3\gamma_3$	$\xi_1\alpha_1 + \xi_1\xi_2\alpha_2 + \xi_1\xi_3\alpha_3$
2	2	$\xi_1\gamma_4 + \xi_3\gamma_5 + \xi_1\xi_3\gamma_6$	$\xi_2\alpha_4 + \xi_2\xi_3\alpha_5 + \xi_1\xi_2\alpha_6$
3	3	$\xi_1\gamma_7 + \xi_2\gamma_8 + \xi_1\xi_2\gamma_9$	$\xi_3\alpha_7 + \xi_2\xi_3\alpha_8 + \xi_1\xi_3\alpha_9$
1	2	$\xi_3\gamma_{10}$	0
2	3	$\xi_1\gamma_{12}$	0
1	3	$\xi_2\gamma_{14}$	0
2	1	$\xi_3\gamma_{11}$	0
3	2	$\xi_1\gamma_{13}$	0
3	1	$\xi_2\gamma_{15}$	0

The interpolates for $\widetilde{\boldsymbol{P}}$ and $\widetilde{\boldsymbol{F}}$ in the physical space are obtained by substituting (3.9) into (3.10), resulting in

$$\widetilde{\boldsymbol{F}}(\boldsymbol{\varphi}) = \boldsymbol{\gamma}_0 + \frac{1}{j(\xi)} \boldsymbol{F}_0 \boldsymbol{T} \left[\mathcal{E}_1(\boldsymbol{\xi}, \boldsymbol{\gamma}) - \mathcal{E}_2(\boldsymbol{\xi}, \boldsymbol{\alpha}) \right] \boldsymbol{T}^T \tag{3.12}$$

$$\widetilde{\boldsymbol{P}}(\boldsymbol{\varphi}) = \boldsymbol{\beta}_0 + \boldsymbol{F}_0^{-T} \boldsymbol{T}^{-T} \mathcal{E}_1(\boldsymbol{\xi}, \boldsymbol{\beta}) \boldsymbol{T}^{-1} \tag{3.13}$$

where

$$\boldsymbol{\gamma}_0 = \boldsymbol{T}^{-1} \widetilde{\boldsymbol{\gamma}}_0 \boldsymbol{T}^{-T} \quad \text{and} \quad \boldsymbol{\beta}_0 = \boldsymbol{T}^T \widetilde{\boldsymbol{\beta}}_0 \boldsymbol{T}$$

3.2. Mixed-Enhanced Deformation Gradient

By isolating the equations associated with the first variation of the first Piola-Kirchhoff stress tensor $\widetilde{\boldsymbol{P}}$ in (2.9) we may solve for the element parameters of the mixed-enhanced deformation gradient $\widetilde{\boldsymbol{F}}$. Recall $(2.9)_3$

$$\int_{\Omega_e} \text{tr} \left[\delta \widetilde{\boldsymbol{P}}^T \left(\text{Grad}\,[\boldsymbol{\varphi}] - \widetilde{\boldsymbol{F}} \right) \right] \, dV = 0 \, . \tag{3.14}$$

Substitution of (3.12) and (3.13) into (3.14) and noting (3.11) yields

$$\begin{gathered} \int_{\Omega_e} \text{tr} \left[\delta \boldsymbol{\beta}_o^T \left(\text{Grad}\,[\boldsymbol{\varphi}] - \boldsymbol{\gamma}_o \right) \right] \, dV = 0 \\ \int_{\Omega_e} \text{tr} \left[\mathcal{E}_1^T(\boldsymbol{\xi}, \delta\boldsymbol{\beta}) \left(\boldsymbol{T}^{-1} \boldsymbol{F}_0^{-1} (\text{Grad}\,[\boldsymbol{\varphi}] - \boldsymbol{\gamma}_0) \boldsymbol{T}^{-T} - \frac{1}{j(\xi)} \mathcal{E}_1(\boldsymbol{\xi}, \boldsymbol{\gamma}) \right) \right] \, dV = 0 \end{gathered} \tag{3.15}$$

Regarding $\delta\boldsymbol{\beta}_0$ and $\delta\boldsymbol{\beta}$ as independent of the arguments within the integrand and the limits of integration we obtain $\boldsymbol{\gamma}_0$ as

$$\boldsymbol{\gamma}_0 = \frac{1}{\Omega_e} \int_{\Omega_e} \text{Grad}\,[\boldsymbol{\varphi}] \, dV = \boldsymbol{F}_0 \, . \tag{3.16}$$

and cast $(3.15)_2$ as

$$\int_{\Omega_e} \overline{\boldsymbol{E}}_1^T \left(\boldsymbol{E}_3 - \frac{1}{j} \boldsymbol{E}_1 \boldsymbol{\gamma} \right) \, dV = 0 \, . \tag{3.17}$$

In (3.17) we have defined the following operators which enable a mapping between tensors and matrices

$$\mathcal{E}_1(\boldsymbol{\gamma}) \rightarrow \boldsymbol{E}_1 \boldsymbol{\gamma} \, , \quad \mathcal{E}_1(\boldsymbol{\beta}) \rightarrow \overline{\boldsymbol{E}}_1 \boldsymbol{\beta} \quad \text{and} \quad \boldsymbol{T}^{-1} \boldsymbol{F}_0^{-1} (\text{Grad}\,[\boldsymbol{\varphi}] - \boldsymbol{F}_0) \boldsymbol{T}^{-T} \rightarrow \boldsymbol{E}_3 \, . \tag{3.18}$$

For two dimensions

$$\boldsymbol{E}_1 = \begin{bmatrix} \xi_2 & 0 \\ 0 & \xi_1 \\ 0 & 0 \\ 0 & 0 \end{bmatrix} \quad \text{and} \quad \overline{\boldsymbol{E}}_1 = \begin{bmatrix} \xi_2 & 0 \\ 0 & \xi_1 \\ 0 & 0 \\ 0 & 0 \end{bmatrix} \, . \tag{3.19}$$

Grouping terms in (3.17) and solving for the element parameter $\boldsymbol{\gamma}$ gives

$$\boldsymbol{\gamma} = \boldsymbol{G}^{-1} \boldsymbol{g} \tag{3.20}$$

where

$$\boldsymbol{g} = \int_{\Omega_e} \overline{\boldsymbol{E}}_1^T \boldsymbol{E}_3 \, dV \quad \text{and} \quad \boldsymbol{G} = \int_{\square} \overline{\boldsymbol{E}}_1^T \boldsymbol{E}_1 \, d\square \, . \tag{3.21}$$

Remark 3.3.

1. Using the interpolations from the previous section results in a diagonal form for $\boldsymbol{G}$. This simplies the solution of the element parameters $\boldsymbol{\gamma}$ to a set of scalar decoupled equations.
2. Note orthogonality of $\mathcal{E}_1$ and $\mathcal{E}_2$ is assumed by $(3.11)_3$. In KASPER & TAYLOR [1997] an alternative formulation for constructing $\mathcal{E}_1$ and $\mathcal{E}_2$ to automatically satisfy the orthogonality condition is presented. However, in this case $(3.11)_{1,2}$ may not hold in general.
3. From the condition $(3.11)_2$ the resulting enhanced part of the deformation gradient will inherit the same properties provided any operators multipling it are constant, $\int_{\Omega_e} \boldsymbol{F}_{enh}\boldsymbol{A}_0 \; dV = 0$ with $\boldsymbol{A}_0 = constant$. Thus the consistency condition or patch test set forth in SIMO *et al.*, [1993] is satified.
4. The stability condition set forth in SIMO & RIFAI, [1990] and SIMO *et al.*, [1993] places the restriction that the conforming and enhanced spaces be independent is satisfied by the choice of interpolations found in Tables 3.1 and 3.2, i.e. the mappings are disjoint.

3.3. Variational Stress Recovery

By isolating $(2.9)_2$ we may solve for the element parameters of the mixed stress, $\widetilde{\boldsymbol{P}}$. Recall $(2.9)_2$

$$\int_{\Omega_e} \delta\widetilde{\boldsymbol{F}} \cdot \left(\boldsymbol{P} - \widetilde{\boldsymbol{P}}\right) \; dV = 0 \tag{3.22}$$

where

$$\boldsymbol{P} = \frac{\partial W}{\partial \widetilde{\boldsymbol{F}}} \tag{3.23}$$

Substitution of (3.12) and (3.13) into (3.22) and noting (3.11) we arrive at

$$\begin{aligned} \int_{\Omega_e} \text{tr} \; \left[\delta\boldsymbol{\gamma}_0^T(\boldsymbol{P} - \boldsymbol{\beta}_0)\right] \; dV = 0 \\ \int_{\Omega_e} \text{tr} \; \left[\frac{1}{\tilde{J}}\mathcal{E}_1^T(\delta\boldsymbol{\gamma})\left(\boldsymbol{T}^T(\boldsymbol{P} - \boldsymbol{\beta}_0)\boldsymbol{T} - \mathcal{E}_1(\boldsymbol{\beta})\right)\right] \; dV = 0 \; . \end{aligned} \tag{3.24}$$

Regarding $\delta\boldsymbol{\gamma}_0$ and $\delta\boldsymbol{\gamma}$ as independent of the arguments within the integrand and the limits of integration we may obtain $\boldsymbol{\beta}_0$ as

$$\boldsymbol{\beta}_0 = \frac{1}{\Omega_e}\int_{\Omega_e} \boldsymbol{P} \; dV := \boldsymbol{P}_0 \tag{3.25}$$

and cast $(3.24)_2$ as

$$\int_{\square} \boldsymbol{E}_1^T \left\{\boldsymbol{E}_5 - \overline{\boldsymbol{E}}_1\boldsymbol{\beta}\right\} \; d\square = 0 \tag{3.26}$$

where we have defined the following operators which enable a mapping between tensors to a matrices

$$\boldsymbol{T}^T \boldsymbol{F}_0 (\boldsymbol{P} - \boldsymbol{P}_0) \boldsymbol{T} \rightarrow \boldsymbol{E}_5 \ . \tag{3.27}$$

Grouping terms in (3.26) and solving for the element parameter $\boldsymbol{\beta}$ gives

$$\boldsymbol{\beta} = \boldsymbol{G}^{-1} \boldsymbol{h} \quad \text{where} \quad \boldsymbol{h} = \int_{\square} \boldsymbol{E}_1^T \boldsymbol{E}_5 \ d\square \ . \tag{3.28}$$

The variationally recoverable stress becomes

$$\widetilde{\boldsymbol{P}} = \boldsymbol{\beta}_0 + \boldsymbol{F}_0^{-T} \boldsymbol{T}^{-T} \mathcal{E}_1(\boldsymbol{\xi}, \boldsymbol{\beta}) \boldsymbol{T}^{-1} \ . \tag{3.29}$$

Remark 3.4.

1. The variational stresses developed above are used for postprocessing only and are not needed for the construction of the residual or tangent.

3.4. Residual and Tangent

By construction, the substitution of (3.12) and (3.13) into (2.6) renders the second term of (2.6) zero, hence we may express a modified functional $\widehat{\Pi}$ as

$$\widehat{\Pi}(\boldsymbol{u}, \widetilde{\boldsymbol{F}}) = \int_{\Omega} W(\widetilde{\boldsymbol{F}}) \ dV + \Pi_{ext}(\boldsymbol{\varphi}) \tag{3.30}$$

The stationary condition of $\widehat{\Pi}$ yields a reduced set of nonlinear equations, which may be expressed (neglecting the external loads) as

$$\delta \widehat{\Pi} = \int_{\Omega} \frac{\partial W}{\partial \widetilde{\boldsymbol{F}}} : \delta \widetilde{\boldsymbol{F}} \ dV \quad \Rightarrow \quad \{ \, \delta \boldsymbol{u}^T \quad \delta \boldsymbol{\alpha}^T \, \} \int_{\Omega} \left\{ \begin{array}{c} \boldsymbol{R}_u \\ \boldsymbol{R}_\alpha \end{array} \right\} \ dV = 0 \ . \tag{3.31}$$

To solve the mixed boundary value problem the above nonlinear residual equations, $\boldsymbol{R}_u$ and $\boldsymbol{R}_\alpha$ are linearized and solved by a Newton method as a sequence of linearized problems. Hence, linearizing (3.31) we obtain

$$\begin{aligned} d(\delta \widehat{\Pi}) = & \int_{\Omega} d\widetilde{\boldsymbol{F}} : \frac{\partial^2 W}{\partial \widetilde{\boldsymbol{F}}^2} : \delta \widetilde{\boldsymbol{F}} + \frac{\partial W}{\partial \widetilde{\boldsymbol{F}}} : d(\delta \widetilde{\boldsymbol{F}}) \ dV \\ & \Rightarrow \quad \{ \, \delta \boldsymbol{u}^T \quad \delta \boldsymbol{\alpha}^T \, \} \int_{\Omega} \left[\begin{array}{cc} \boldsymbol{K}_{uu} & \boldsymbol{K}_{u\alpha} \\ \boldsymbol{K}_{\alpha u} & \boldsymbol{K}_{\alpha\alpha} \end{array} \right] \ dV \left\{ \begin{array}{c} d\boldsymbol{u} \\ d\boldsymbol{\alpha} \end{array} \right\} \end{aligned} \tag{3.32}$$

Noting that the variations $\delta \boldsymbol{u}$ and $\delta \boldsymbol{\alpha}$ in (3.31) are arbitrary we obtain the finite element residual vectors

$$\begin{aligned} &\mathop{\mathbf{A}}_{e=1}^{nelm} \left[\boldsymbol{f}_{int}(\boldsymbol{u}_e, \boldsymbol{\alpha}_e) - \boldsymbol{f}_{ext}(\boldsymbol{u}_e) \right] = \mathbf{0} \\ &\boldsymbol{f}_{enh}(\boldsymbol{u}_e, \boldsymbol{\alpha}_e) = \mathbf{0}, \quad (e = 1, 2, \ldots, nelm) \ . \end{aligned} \tag{3.33}$$

where

$$\boldsymbol{f}_{int}(\boldsymbol{u}_e, \boldsymbol{\alpha}_e) = \int_{\Omega_e} \boldsymbol{R}_u \ dV \ , \qquad \boldsymbol{f}_{enh}(\boldsymbol{u}_e, \boldsymbol{\alpha}_e) = \int_{\Omega_e} \boldsymbol{R}_\alpha \ dV \tag{3.34}$$

$\boldsymbol{f}_{ext}$ is the standard external force vector

$$\boldsymbol{f}_{ext}(\widehat{\boldsymbol{u}}_e) = \int_{\Omega_e} \rho_o \boldsymbol{N}^T \boldsymbol{b} \ dV + \int_{\Gamma_e} \boldsymbol{N}^T \bar{\boldsymbol{t}} \ dS \tag{3.35}$$

and $\mathbf{A}$ denotes the finite element assembly operator. With the aid of (3.32) linearizing (3.33) about an intermediate state $(\boldsymbol{u}_e^{(k)}, \boldsymbol{\alpha}_e^{(k)})$ yields

$$\begin{aligned} L[\boldsymbol{f}_{int}] &= \boldsymbol{f}_{int}^{(k)} + \boldsymbol{K}_{uu}^{(k)} \ d\boldsymbol{u}_e + \boldsymbol{K}_{u\alpha}^{(k)} \ d\boldsymbol{\alpha}_e \\ L[\boldsymbol{f}_{enh}] &= \boldsymbol{f}_{enh}^{(k)} + \boldsymbol{K}_{\alpha u}^{(k)} \ d\boldsymbol{u}_e + \boldsymbol{K}_{\alpha\alpha}^{(k)} \ d\boldsymbol{\alpha}_e \ . \end{aligned} \tag{3.36}$$

From $(3.33)_2$ we observe that $(3.36)_2$ may be solved at an element level. Accordingly,

$$d\boldsymbol{\alpha}_e = - \left[\boldsymbol{K}_{\alpha\alpha}^{(k)} \right]^{-1} \left(\boldsymbol{f}_{enh}^{(k)} + \boldsymbol{K}_{\alpha u}^{(k)} \ d\boldsymbol{u}_e \right) \ . \tag{3.37}$$

Substituting (3.37) into $(3.36)_1$ we arrive at an equivalent displacement model involving only the nodal displacement vector at the global level

$$\boldsymbol{K}^{(k)} \ d\boldsymbol{u} = \boldsymbol{R}^{(k)} \tag{3.38}$$

where

$$\begin{aligned} \boldsymbol{K}^{(k)} &= \mathop{\mathbf{A}}_{e=1}^{nelm} \left[\boldsymbol{K}_{uu} - \boldsymbol{K}_{u\alpha} \ (\boldsymbol{K}_{\alpha\alpha})^{-1} \ \boldsymbol{K}_{\alpha u} \right]_e^{(k)} \\ \boldsymbol{R}^{(k)} &= \mathop{\mathbf{A}}_{e=1}^{nelm} \left[\boldsymbol{f}^{ext} - \boldsymbol{f}^{int} + \boldsymbol{K}_{u\alpha} (\boldsymbol{K}_{\alpha\alpha})^{-1} \ \boldsymbol{f}^{enh} \right]_e^{(k)} \ . \end{aligned}$$

The system (3.38) is solved and the unknown fields are updated by

$$\begin{aligned} \boldsymbol{u}_e^{(k+1)} &= \boldsymbol{u}_e^{(k)} + d\boldsymbol{u}_e \\ \boldsymbol{\alpha}_e^{(k+1)} &= \boldsymbol{\alpha}_e^{(k)} + d\boldsymbol{\alpha}_e \ . \end{aligned} \tag{3.39}$$

The process is repeated within a particular time step t_n until convergence of the $(k+1)^{th}$ iterate is obtained, the solution is then advanced to the next time step t_{n+1}.

Remark 3.5.

1. To obtain $d\boldsymbol{\alpha}$ in (3.37) one can either recompute the array for each element at each global iterate k or store the arrays associated with the k global iterate. This storage is in addition to any other data needed for the element such as for inelastic internal variables. For three dimensional problems with fine meshes demand on memory or disk becomes significant.
2. An alternative algorithm, introduced by SIMO *et al.*, [1993], for obtaining the element parameters $\boldsymbol{\alpha}$ is outlined in Appendix B of KASPER & TAYLOR [1997] which circumvents the large demand on memory and requires storage of only the element parameters, $\boldsymbol{\alpha}$ from the previous global iterate.

4. Numerical Simulations

In this section we investigate the performance of the formulation described above. Specifically, we show the locking free response in the incompressible limit and improved performance in bending dominated problems. To assess the performance of our formulation several representative simulations are presented below in the setting of plane strain and three dimensional hyperelasticity. Comparisons are made with different element formulations.

The element formulations considered are:

H1 This hexahedral element is a standard eight-node displacement formulation using tri-linear interpolation functions and a standard 8-pt quadrature rule, its two dimensional counterpart is denoted as **Q1**.

H1/E9 This hexahedral element is an enhanced formulation with 9 enhanced modes and utilizes tri-linear interpolation functions and a standard 8-pt quadrature rule, see SIMO & ARMERO [1992] for further details, its two dimensional counterpart is denoted as **Q1/E4**.

H1/E12 This hexahedral element is an enhanced formulation with 12 enhanced modes and utilizes modified tri-linear interpolation functions and a special 9-pt quadrature rule, also described in SIMO *et al.* [1993].

H1/E21 This hexahedral element is an enhanced formulation with 21 enhanced modes and utilizes tri-linear interpolation functions and a standard 8-pt quadrature rule, see ANDELFINGER, [1992] for further details.

H1/ME9 The new mixed-enhanced formulation with 9 enhanced modes, standard tri-linear interpolation functions, and standard 8-pt quadrature rule, its two dimensional counterpart is denoted as **Q1/ME2**.

For the simulations presented we consider the elastic response for two stored energy functions, namely a compressible neo-Hookean material model and a generalized Ogden material model. The neo-Hookean material model, MOONY [19] is characterized by the stored energy density

$$W = \frac{1}{2}\lambda(\ln J)^2 + \frac{1}{2}\mu(\operatorname{tr} C - 3 - 2\ln J) \tag{4.1}$$

while the stored energy density for the Ogden model, OGDEN [1984] is

$$W = \sum_{i=1}^{n} \left[\frac{\mu_i}{\alpha_i} (\lambda_1^{\alpha_i} + \lambda_2^{\alpha_i} + \lambda_3^{\alpha_i}) - \mu_i \ln J \right] + \frac{\lambda}{4} \left(J^2 - 1 - 2 \ln J \right) \tag{4.2}$$

where J is the determinate of the deformation gradient, $\boldsymbol{C} = \boldsymbol{F}^T \boldsymbol{F}$ is the Cauchy-Green stress tensor, λ and μ are the Lame type parameters from linear elasticity and μ_i and α_i are material parameters. From (4.1) and (4.2) we may obtain the stress and the material tensor by standard operations.

4.1. Eigenvalue Analysis

To appraise the behavior of the elements above at the nearly incompressible limit an eigenvalue analysis for a single finite element is performed. The two configurations considered are depicted in Figure 4.1.1. For both, the assumed mechanical properties are λ = 1.67 E+05 and $\mu = \frac{1}{3}$. The analysis is performed at the reference state and Table 4.1.1 and 4.1.2 include only the 18 non-zero eigenvalues, i.e. the 6 rigid body modes are excluded. Values five orders of magnitude greater than the tabulated values are denoted by the ∞ symbol. For a locking-free element only one mode, corresponding to the dilatational mode, should tend toward infinity as $\frac{\lambda}{\mu} \to \infty$. If any additional modes tend toward infinity the element will exhibit volumetric locking.

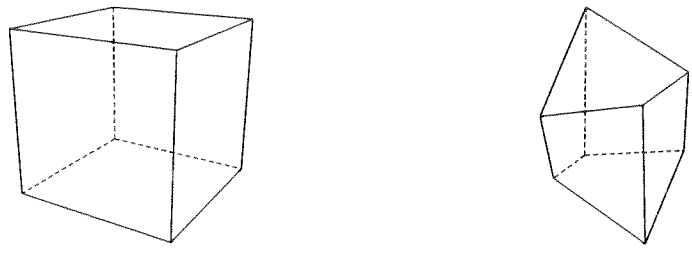

Figure 4.1.1 Undistorted and Distorted Configurations of a Hexahedran

Table 4.1.1 Eigenvalues for a Nearly Incompressible 8-Node Regular Hexahedral Element

Mode	H1	H1/E9	H1/E12	H1/E21	H1/ME9
1	5.5556E-02	5.5556E-02	5.5556E-02	5.5556E-02	5.5556E-02
2	5.5556E-02	5.5556E-02	5.5556E-02	5.5556E-02	5.5556E-02
3	1.6667E-01	1.1111E-01	1.1111E-01	5.5556E-02	5.5556E-02
4	1.6667E-01	1.1111E-01	1.1111E-01	5.5556E-02	5.5556E-02
5	1.6667E-01	1.1111E-01	1.1111E-01	5.5556E-02	5.5556E-02
6	2.2222E-01	2.2222E-01	1.1111E-01	1.1111E-01	1.1111E-01
7	3.3333E-01	3.3333E-01	1.1111E-01	1.1111E-01	1.1111E-01
8	3.3333E-01	3.3333E-01	1.1111E-01	1.1111E-01	1.1111E-01
9	3.3333E-01	3.3333E-01	2.2222E-01	2.2222E-01	2.2222E-01
10	3.3333E-01	3.3333E-01	3.3333E-01	3.3333E-01	3.3333E-01
11	3.3333E-01	3.3333E-01	3.3333E-01	3.3333E-01	3.3333E-01
12	∞	3.3333E-01	3.3333E-01	3.3333E-01	3.3333E-01
13	∞	3.3333E-01	3.3333E-01	3.3333E-01	3.3333E-01
14	∞	3.3333E-01	3.3333E-01	3.3333E-01	3.3333E-01
15	∞	∞	3.3333E-01	3.3333E-01	3.3333E-01
16	∞	∞	3.3333E-01	3.3333E-01	3.3333E-01
17	∞	∞	3.3333E-01	3.3333E-01	3.3333E-01
18	∞	∞	∞	∞	∞

Table 4.1.2 Eigenvalues for Nearly Incompressible 8-Node Distorted Hexahedral Element

Mode	H1	H1/E9	H1/E12	H1/ME9
1	3.6273E-02	3.0720E-02	3.3857E-02	3.3108E-02
2	7.5142E-02	5.5337E-02	5.6785E-02	3.9517E-02
3	1.3489E-01	1.0233E-01	8.0446E-02	6.6768E-02
4	1.6698E-01	1.3401E-01	1.0274E-01	7.4400E-02
5	1.9041E-01	1.4662E-01	1.0760E-01	8.2449E-02
6	2.1365E-01	1.9201E-01	1.2176E-01	8.9910E-02
7	2.5897E-01	2.1791E-01	1.3636E-01	1.0429E-01
8	3.2395E-01	2.5554E-01	1.4528E-01	1.5998E-01
9	3.8442E-01	2.9852E-01	1.8486E-01	1.7127E-01
10	4.0333E-01	3.1738E-01	2.3426E-01	2.2994E-01
11	2.1370E+01	3.8075E-01	2.6414E-01	2.6744E-01
12	∞	4.3302E-01	2.9215E-01	3.0429E-01
13	∞	4.8680E-01	3.4335E-01	3.1834E-01
14	∞	3.8748E+01	3.7548E-01	3.4756E-01
15	∞	∞	3.8995E-01	4.2667E-01
16	∞	∞	4.6811E-01	4.4534E-01
17	∞	∞	5.2791E-01	5.0957E-01
18	∞	∞	∞	∞

For the two dimension formulation an eigenvalue analysis is used to track the two hourglass modes for the two material models under various values of stretch. Figure 4.1.1 illustrates the configuration and stress state for the simulations.

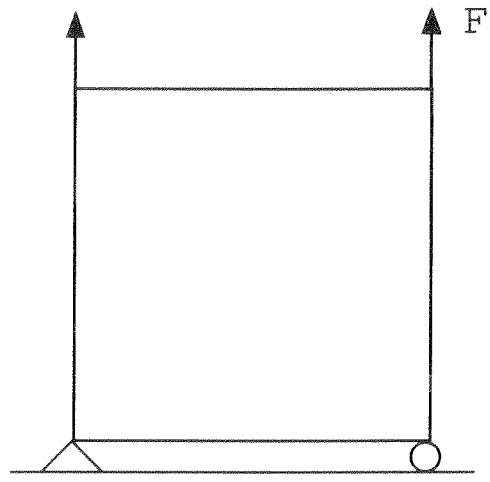

Figure 4.1.1 Undistorted Configurations for Eigenvalue Analysis

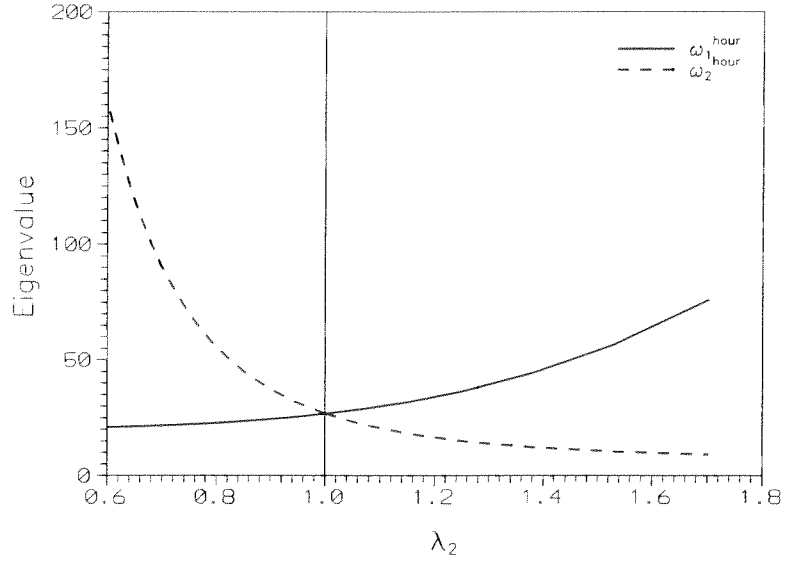

Figure 4.1.2 neo-Hookean Material Model with $\lambda = 10^5$ and $\mu = 20$.

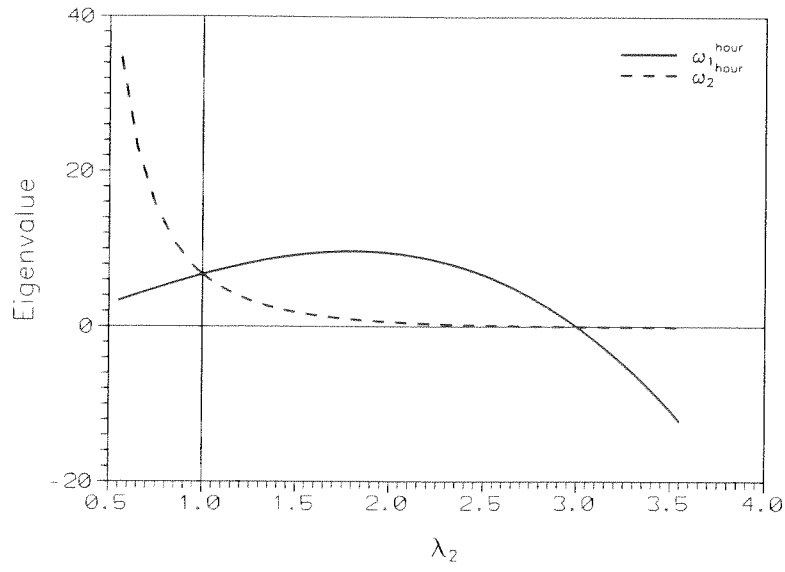

Figure 4.1.3 Ogden Material Model with $\lambda = 10^5$, $\mu = 20$ and $\alpha = 0.5$.

Figures 4.1.2 and 4.1.3 depict the two eigenvalues corresponding to the bending (hourglass) modes for the linearized system. Note, for compression the eigenvalues remain positive for all values of stretch, λ_2, correcting the appearence of spurious modes in compression as observed by WRIGGERS & REESE [1996]. As shown in ARMERO [1996], a limit point exists for the Ogden model used above at a stretch of $\lambda = 3$. Values of stretch greater than this critical value result in a negative axial stiffness and a corresponding negative stretching eigenvalue. The second hourglass mode in Figure 4.1.3 becomes negative just after the appearence of this critical value. Thus, a tendency for elements to have large hourglass modes may still be possible.

4.2. Objectivity

In this section we examine the effect of a super-posed rigid body motion on the deformed configuration to ensure the formulation is frame-invariant. Frame-invariance will lead to a finite element method which preserves the objectivity of the constitutive equations, see GLASER & ARMERO [1995]. We first consider a plane strain strip plate under the external action of bending moment at the free end. The simulation is performed and the normal component of the *2nd* Piola-Kirchhoff stress in the axial direction is reported in Figure 4.2.1. The body is then subjected to a super-posed rigid body rotation of 60° and the stresses are recomputed in the new configuration as depicted in Figure 4.2.2. From Figures 4.2.1 and 4.2.2 we see that the resulting formulation is objective under super-posed rigid body motion and thus preserves the objectivity of the consitutive equations.

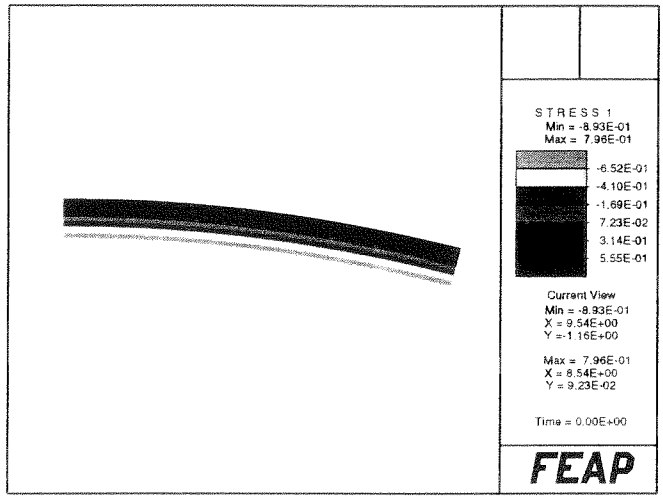

Figure 4.2.1 Distorted Configuration Before SRBM

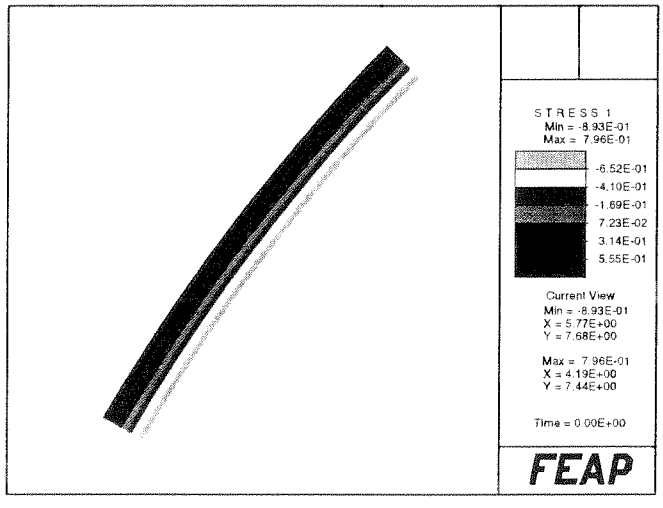

Figure 4.2.2 Distorted Configuration After SRBM

4.3. Homogeneous Compression of a Billet

To determine the performance of the present formulation in highly strained regimes, we consider the compression of a plane-strain billet. The initial configuration is a unit square consisting of 256 four node quadralaterial elements. Due to symmetry, only one-half of the structure was analyzed. The billet is loaded via displacement control on the upper edge, while the lower edge is restrained against translation. The vertical motion of the billet on the lower edge is enforced by a simple node-on-node penalty formulation with a penalty parameter of 1E+06. A neo-Hookean material model was used for the simulation with $\lambda =$ 4E+04 and $\mu = 80.2$. Figure 4.3.1 depicts the progression of the deformation.

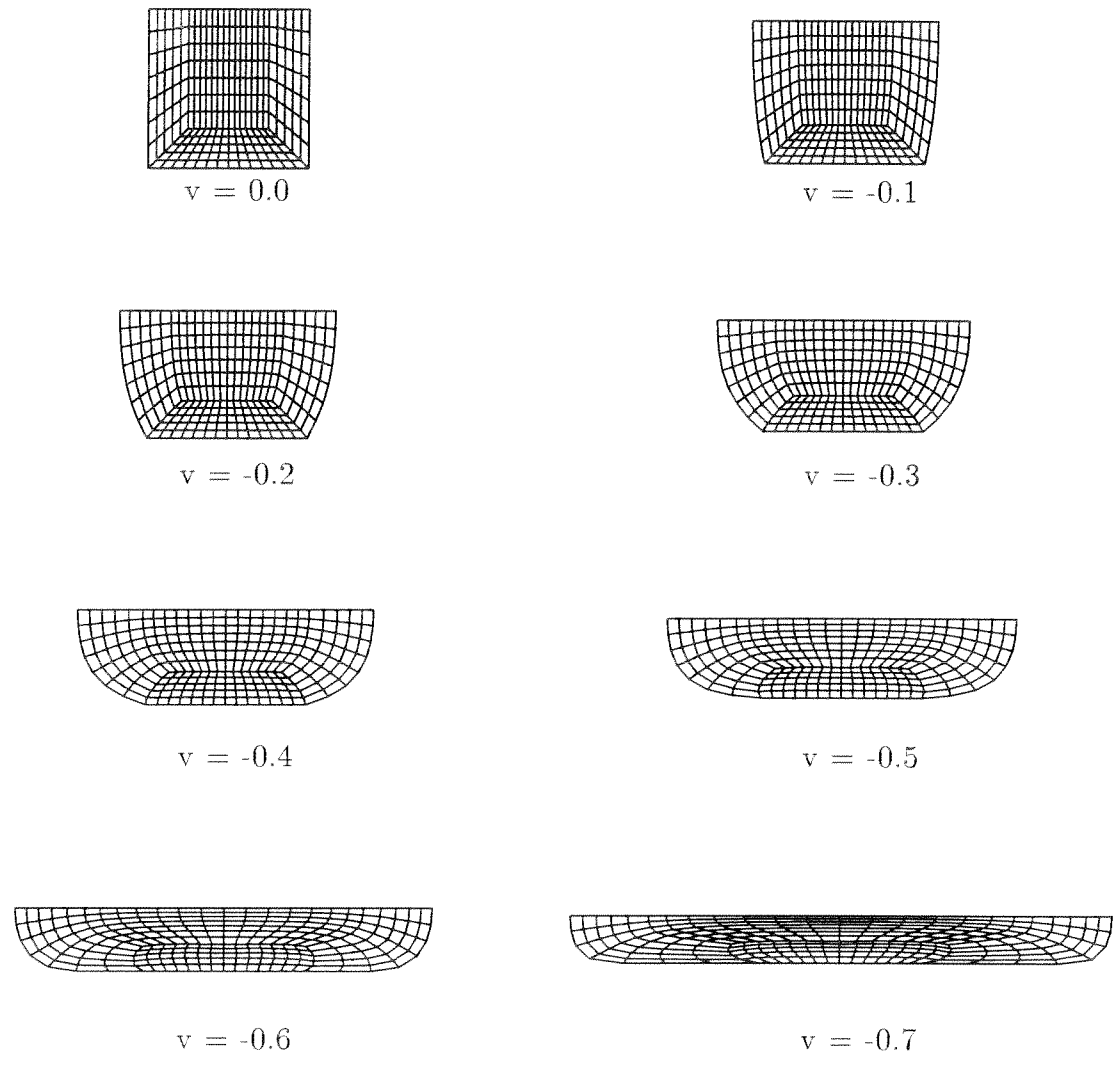

Figure 4.3.1 Deformed configurations at various prescribed displacements.

4.4. Indentation Problem

Another simulation for highly strained regimes is the indentation of a rectangular block. The initial configuration consists of a 2×1 block with 200 four node quadralateral elements. The block is loaded via displacement control over one-half of the upper edge, while the lower edge is restrained against any motion. The sides of the block are allowed to translate freely in the vertical direction, but restrained horizontally. A neo-Hookean material model with $\lambda = 4\text{E}{+}04$ and $\mu = 80.2$ was used. Figure 4.4.1 depicts the initial and final configurations.

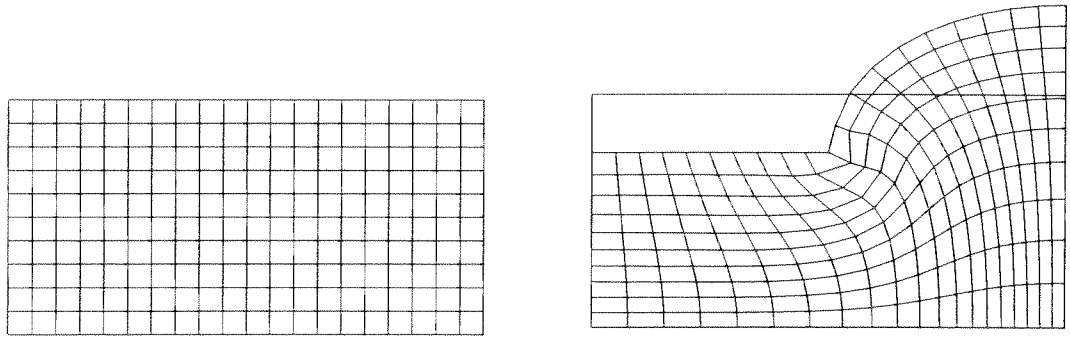

Figure 4.4.1 Initial and final configurations

4.5. Strip Plate

In this simulation we consider the extension of a perforated sheet. The reference geometry is a 20×20 square domain with a 6 diameter circular hole at the center with a total of 800 elements. Due to symmetry only one-quarter of the mesh was modeled. The simulation was performed using four node plane strain quadrilaterals and eight node hexahedral elements (with one element in the thickness direction). The perforated sheet is clamped and loaded horizontally (via displacement control) along the two outer vertical boundaries, while the outer horizontal boundaries are allowed to translate freely. A neo-Hookean material model with λ = 4E+04 and μ = 80.2 was used. Figure 4.5.1 depicts the initial configuration, while Figures 4.5.2 thru 4.5.4 depict the deformed configurations for a plane strain and three dimensional deformation state.

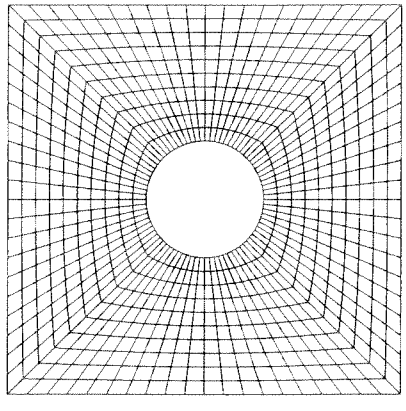

Figure 4.5.1 Reference configuration.

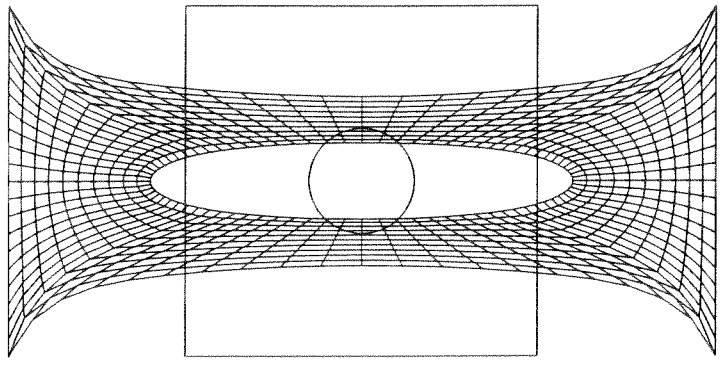

Figure 4.5.2 Final configuration using a plane strain model.

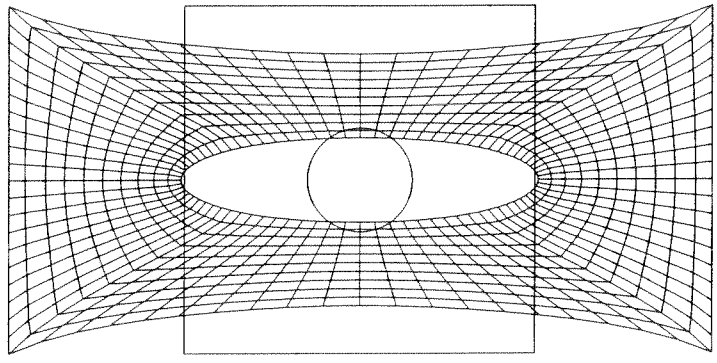

Figure 4.5.3 Final configuration using a three dimensional model.

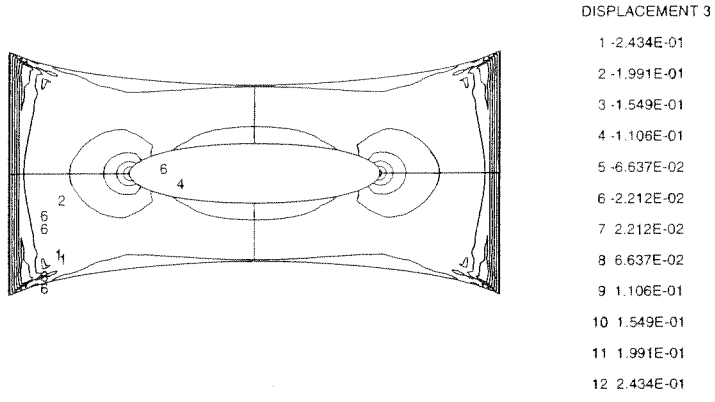

Figure 4.5.4 Displacement contours of the deformed three dimensional model.

4.6. Upsetting of a Cylindrical Billet

To determine the performance of the present hexahedral element formulation in highly strained regimes, we consider the compression of a three dimensional cylindrical billet.

The initial configuration is a cylinder with a radius, $r = 10$ and a height, $h = 15$ consisting of 459 eight node hexahedral elements. The billet is loaded via displacement control on the upper edge, while the lower edge is restrained against translation. A neo-Hookean material model was used for the simulation with $\lambda =$ 1E+04 and $\mu = 10$. Figure 4.6.1 depicts the progression of the deformation.

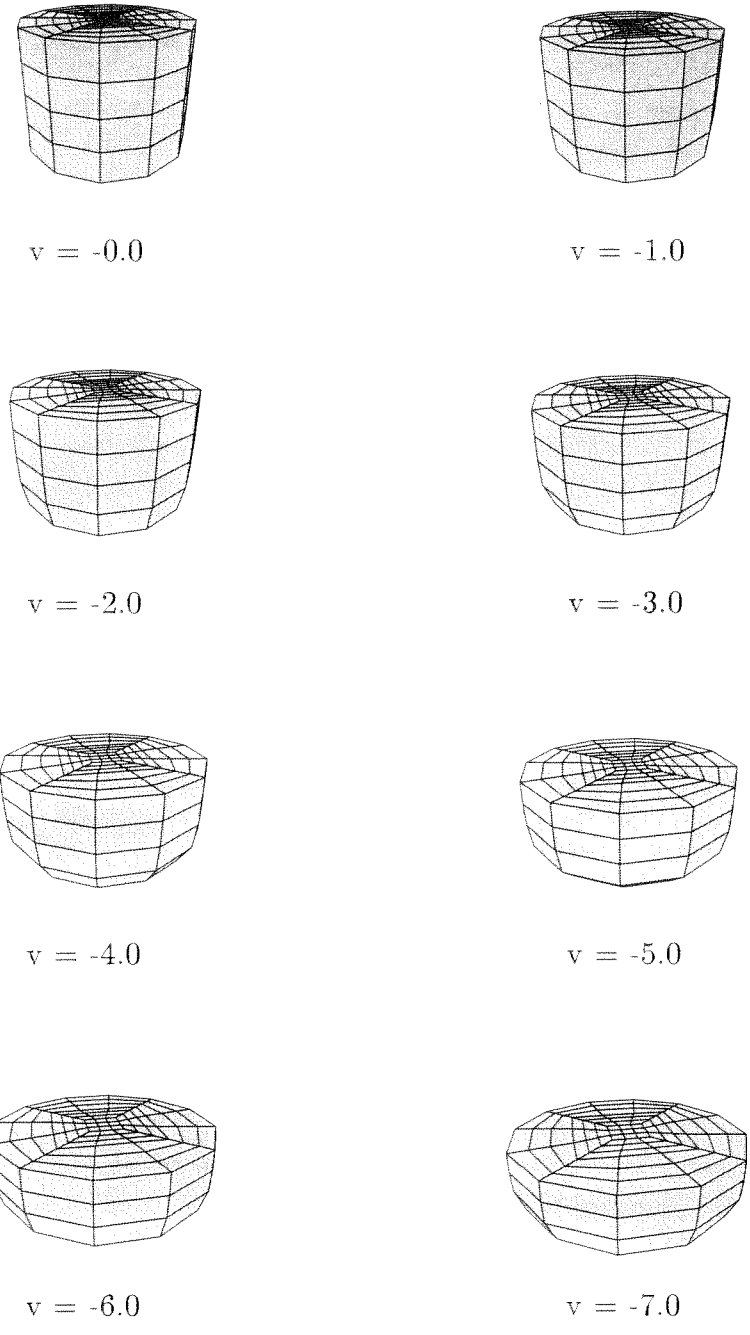

Figure 4.6.1 Deformed configurations at various prescribed displacements.

5. Closure

We have presented a new class of *assumed strain* methods employing low order finite elements in the setting of finite deformation problems in hyperelasticity The present methodology circumvents spurious modes in highly compressive regimes in additional to improved coarse mesh accuracy and locking free response in quasi-incompressible regimes. The present formulation also allows for variational stress recovery, which is absent in other enhanced formulations.

The performance exhibited by the Q1/ME2 and H1/ME9 in bending and quasi-incompressible regions offers an attractive methodology for a systematic development of mixed-enhanced finite elements. Further extensions to the present work include: a) introduction of alternative enhanced modes, b) performance evalution of inelastic material models c) introduce alternative interpolatation functions for the first Piola-Kirchhoff stress and the deformation gradient.

References

Amrero, F. [1996], "A Modal Analysis of Finite Deformation Enhanced Strain Finite Elements", UCB/SEMM-96/03 Report, February 1996, University of California at Berkeley.

Andelfinger, U., Ramm, E. & Roehl, D. [1992], "2D- and 3D-Enhanced Assumed Strain Elements and Their Application in Plasticity",*Computational Plasticity, Proceedings of the 4th International Conference,*, ed. D. Owen, E. Onate and E. Hinton, 1997-2007, Pineridge Press, Swansea, U.K.

Ciarlet, P.G. [1988], *Mathematical Elasticity*, Vol I, North-Holland.

Crisfield, M.A., Moita, G.F., Jelenic, G. & Lyons, L.P.R. [1995], "Enahnced Lower-Order Element Formulations for Large Strains", *Computational Mechanics*, **17**, 62-73.

Glaser, S. & Amrero, F. [1995], "Recent Developments in Enhanced Strain Finite Elements", UCB/SEMM-95/13 Report, December 1995, University of California at Berkeley.

Hughes [1987], *The Finite Element Method*, Prentice-Hall, Englewood Cliff, N.J.

Kasper, E.P. & Taylor, R.L. [1997], "A Mixed-Enhanced Strain Method: Linear Problems", UCB/SEMM-97/02 Report, Feburary 1997, University of California at Berkeley.

KORELC, J & WRIGGERS, P. [1996], "Consistent Gradient Formulation for a Stable Enhanced Strain Method for Large Deformations", *Engineering Computations*, **13-1**, 103-123.

OGDEN, R.W. [1984], "Non-Linear Elastic Deformations", Ellis Horwood Limited.

REESE, S. & WRIGGERS, P. [1995], "A Finite Element Method for Stability Problems in Finite Elasticity", *International Journal of Numerical Methods in Engineering*, **38**, 1171-1200.

SIMO, J.C. & RIFAI, M.S. [1990], "A Class of Mixed Assumed Strain Methods and The Method of Incompatible Modes", *International Journal of Numerical Methods in Engineering*, **29**, 1595-1638.

SIMO, J.C. & ARMERO, F. [1992], "Geometrically Non-linear Enhanced Strain Mixed Methods and the Method of Incompatible Modes", *International Journal of Numerical Methods in Engineering*, **33**, 1413-1449.

SIMO, J.C., ARMERO, F. & TAYLOR, R.L. [1993], "Improved versions of assumed enhanced strain tri-linear elements for 3D finite deformation problems", *Computer Methods in Applied Mechanics and Engineering*, **110**, 359-386.

SOKOLNIKOFF, I.S. [1964], *Tensor Analysis Theory and Applications to Geometry and Mechanics of Continua*, John Wiley & Sons, Inc., New York.

TAYLOR, R.L., BERESFORD, P.J. & WILSON, E.L. [1976], "A non-Conforming Element for Stress Analysis", *International Journal of Numerical Methods in Engineering*, **10**, 1211-1219.

WASHIZU, K. [1982], *Variational Methods in Elasticity and Plasticity*, 3rd ed., Pergamon Press.

WILSON, E.L., TAYLOR, R.L., DOHERTY, W.P. & GHABOUSSI, J. [1973], "Incompatible Displacement Models", *Numerical and Computer Methods in Structural Mechanics*, 43.

WRIGGERS, P. & REESE, S. [1996], "A Note on Enhanced Strain Methods for Large Deformations", *Computer Methods in Applied Mechanics and Engineering*, **135**, 201-209.

ZIENKIEWICZ, O.C. & TAYLOR, R.L. [1989], *The Finite Element Method*, Vol 2., 4th ed., McGraw-Hill, London.